Structure of androcam supports specialized interactions with myosin VI

Mehul K. Joshi[a,b], Sean Moran[a,c], Kathleen M. Beckingham[a], and Kevin R. MacKenzie[a,d,1]

[a]Department of Biochemistry and Cell Biology, Rice University, Houston, TX 77005; [b]Department of Medicinal Chemistry and Molecular Pharmacology, Purdue University, West Lafayette, IN 47907; [c]Uniformed Services University of the Health Sciences, Bethesda, MD 20814; and [d]Department of Biology and Biochemistry, University of Houston, Houston, TX 77004

Edited by Thomas D. Pollard, Yale University, New Haven, CT, and approved July 5, 2012 (received for review June 12, 2012)

Androcam replaces calmodulin as a tissue-specific myosin VI light chain on the actin cones that mediate *D. melanogaster* spermatid individualization. We show that the androcam structure and its binding to the myosin VI structural (Insert 2) and regulatory (IQ) light chain sites are distinct from those of calmodulin and provide a basis for specialized myosin VI function. The androcam N lobe noncanonically binds a single Ca^{2+} and is locked in a "closed" conformation, causing androcam to contact the Insert 2 site with its C lobe only. Androcam replacing calmodulin at Insert 2 will increase myosin VI lever arm flexibility, which may favor the compact monomeric form of myosin VI that functions on the actin cones by facilitating the collapse of the C-terminal region onto the motor domain. The tethered androcam N lobe could stabilize the monomer through contacts with C-terminal portions of the motor or recruit other components to the actin cones. Androcam binds the IQ site at all calcium levels, constitutively mimicking a conformation adopted by calmodulin only at intermediate calcium levels. Thus, androcam replacing calmodulin at IQ will abolish a Ca^{2+}-regulated, calmodulin-mediated myosin VI structural change. We propose that the N lobe prevents androcam from interfering with other calmodulin-mediated Ca^{2+} signaling events. We discuss how gene duplication and mutations that selectively stabilize one of the many conformations available to calmodulin support the molecular evolution of structurally and functionally distinct calmodulin-like proteins.

chemical exchange | chemical shift perturbation | EF-hand | NMR

The chief transducer of intracellular Ca^{2+} signals, calmodulin, is ubiquitously expressed and completely conserved across vertebrates; only three of its 148 residues differ between man and *D. melanogaster*. The flexible calmodulin central linker connects two globular lobes, each with two EF-hand motifs and a short antiparallel β sheet (1, 2). Ca^{2+} binding to EF-hand motif side chain and backbone oxygens changes each lobe from a "closed" antiparallel four helix bundle to an "open" conformation that exposes a hydrophobic binding cleft (3, 4). Calmodulin binds hundreds of proteins in many interaction modes (5), but despite this versatility, all metazoans express additional Ca^{2+} binding EF-hand proteins similar to calmodulin. What roles these proteins play in Ca^{2+} signaling are the subject of ongoing research.

We are studying the structure and binding properties of the testis-specific calmodulin-like *D. melanogaster* protein androcam (6), which is conserved across the genus (7), to understand its role as a tissue-specific light chain for myosin VI in fly spermatogenesis (8). In mammals, the light chain calmodulin binds to two myosin VI motifs within the lever arm: the myosin VI-specific Insert 2 sequence and an IQ motif (9, 10). In the Drosophila ovary, calmodulin binds to myosin VI, but in the testis, androcam (and not calmodulin) coimmunoprecipitates with myosin VI (8). Androcam colocalizes with myosin VI at the flat leading edge of specialized structures (actin cones) as they move along the axonemes during spermatid individualization, and this localization is myosin VI–dependent (8). Sequence alignment (Fig. 1) reveals that the C-terminal lobe (C lobe) is more strongly conserved than the N-terminal lobe (N lobe), and although the androcam C lobe binds two Ca^{2+} ions 40-fold more tightly than calmodulin, the N lobe binds weakly to only one Ca^{2+} (11). Androcam interacts with both Insert 2 and IQ regions of Drosophila myosin VI in yeast two-hybrid analysis, but binds more weakly than calmodulin to an Insert 2 peptide (8). These prior studies demonstrate that the proteins are biochemically distinct but fail to illuminate how androcam might preferentially localize to the actin cones or might adjust the properties of myosin VI for its role in spermatogenesis. We identify a unique metal binding site in the N lobe and show that androcam binds to the myosin VI Insert 2 and IQ motifs differently from calmodulin with implications for myosin VI function.

Results

The Androcam N Lobe Binds Ca^{2+} Weakly. Androcam binds Ca^{2+} at two C-lobe high affinity sites (K_Ds of 56 nM and 25 nM) and at a weak N-lobe site with a K_D lower limit of 80 μM (11). To map the residues at the weak site, we monitored NMR chemical shift changes in a $CaCl_2$ titration. We prepared 190 μM androcam at 10 μM free calcium to saturate the C lobe and leave the N lobe >96% vacant if $K_D = 80$ μM. Two-dimensional ^{15}N heteronuclear single quantum coherence (HSQC) spectra revealed chemical shift changes for more than a dozen peaks (Fig. 2 and Fig. S1). Small shift changes for the linker and terminal residues are similar to nonspecific salt effects seen in a control KCl titration. Residues with the largest backbone amide shift changes are near the second EF hand, but residues at the first EF hand also show changes. All residues give single peaks at each titration point, indicating that Ca^{2+} binding is in fast exchange. Peak movements fit a single binding site model with $K_D = 4.1$ mM (Fig. 2), 50-fold weaker than the lower limit determined previously (11). The modest spectral changes indicate that Ca^{2+} binding has a local effect but does not alter the overall N lobe conformation.

Due to cooperativity between the androcam high affinity sites (11) the C lobe will bind two calcium ions even at the low Ca^{2+} levels of resting cells (typically 100 nM) (12), but the weak N-lobe Ca^{2+} affinity means this lobe will be calcium-free across the physiological Ca^{2+} range. Thus, unlike calmodulin, androcam exists as a "saturated C-lobe, calcium-free N-lobe" species from high nM to tens of μM free Ca^{2+}. We determined the structure of this "holo C-lobe, apo N-lobe" form of androcam using NMR samples kept at 10 μM free Ca^{2+} by a Ca^{2+}/citrate buffer (13).

Androcam Has Two Well-Defined Lobes Separated By A Flexible Linker. After resonance assignment (13), we calculated low energy, high quality structures in ARIA 1.2 (14) that satisfy more than 38

Author contributions: M.K.J., K.M.B., and K.R.M. designed research; M.K.J. performed research; M.K.J., S.M., and K.R.M. analyzed data; and M.K.J., K.M.B., and K.R.M. wrote the paper.

The authors declare no conflict of interest.

This article is a PNAS Direct Submission.

[1]To whom correspondence should be addressed. E-mail: krmackenzie@uh.edu.

This article contains supporting information online at www.pnas.org/lookup/suppl/doi:10.1073/pnas.1209730109/-/DCSupplemental.

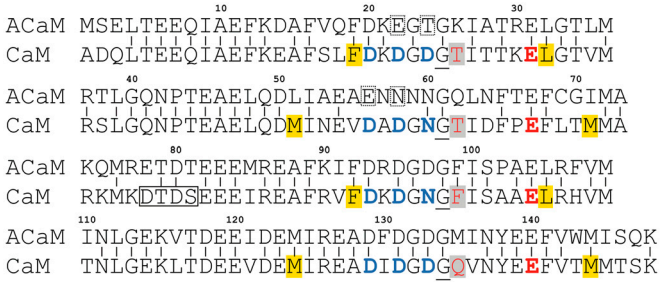

Fig. 1. Androcam and calmodulin sequence alignment. Calmodulin EF-hand residues are blue (red) if one (two) side chain oxygens contact Ca^{2+}, and in gray boxes if the backbone carbonyl oxygen does so. Calmodulin flexible linker residues (2) are boxed, and EF-hand glycines with downfield amide protons are underlined. Androcam residues that deviate from EF-hand motifs are in dotted boxes. Four residues in each calmodulin lobe that contact bound targets (40) are in yellow boxes. The androcam C lobe conserves all these elements, but the N lobe shows changes relative to calmodulin.

restraints per residue (Table S1). Like calmodulin, androcam is bilobed with N- and C-terminal domains structurally uncoupled in solution. Poor superposition of linker residues 75–84 suggests local flexibility, which is supported by low ^{1}H-^{15}N heteronuclear NOE values (<0.6) at residues 77–82, as in calmodulin (2). Both androcam lobes are well defined: The Cα atoms of residues 85–148 superimpose with rmsd of 0.18 Å (Fig. 3*A*), and the Cα atoms of residues 4–74 superimpose with rmsd of 0.23 Å (Fig. 3*B*). Each lobe is well ordered (^{1}H-^{15}N NOE > 0.6) except for loop residues 21, 22, and 115–117.

The Androcam C Lobe Resembles the Ca^{2+}-Calmodulin C Lobe. The androcam C lobe is very similar to the Ca^{2+}-loaded "holo"-calmodulin C lobe (1CLL, Cα rmsd = 1.45 Å; Fig. 3*A*), with helices that lead into and out of the EF loops roughly perpendicular to each other in the open conformation. The DALI server (15) identifies a dozen calmodulin lobes that superimpose on the average androcam C lobe with Cα rmsd < 1.5 Å. Both androcam C-lobe EF hands are consistent with the pentagonal bipyramid Ca^{2+} coordination seen in calmodulin (1), and our structures rule out the possibility that the 40-fold tighter Ca^{2+} binding of the androcam C lobe relative to calmodulin (11) could be caused by protein atoms replacing water as the axial seventh ligand.

The Androcam N Lobe Resembles the Ca^{2+}-Free Calmodulin N Lobe Bound to the Myosin VI IQ Motif. The androcam N lobe adopts an antiparallel four-helix bundle in which the second and fourth helices pack against each other and the first and third helices pack on opposite faces of this core (Fig. 3*B*). Residues 26–28 and 62–64 form an antiparallel β sheet over one end of the helical bundle. Motif residues Asp20, Glu22, and Thr24 of the first EF-hand (Fig. 1) form a pocket, but Glu56, Asn58, and Asn60 of the second EF-hand form a helix and their side chains point away from one another. The androcam N lobe superimposes poorly on the holo-calmodulin N lobe (1CLL, Cα rmsd = 5.09 Å) and on most known calmodulin structures, but it superimposes well on the closed apo-calmodulin N lobe bound to the IQ region of pig myosin VI (16) (3GN4, Cα rmsd = 1.41 Å) (Fig. 3*B*). This similarity suggests that the androcam N lobe could bind the IQ site much like calmodulin. Calmodulin N lobe residues that contact the myosin VI lever arm at the IQ site are mostly conserved in androcam, but residues that differ from calmodulin cluster on the opposite surface of the N lobe (Fig. 3*C*).

The Androcam N Lobe Remains Closed on Binding Ca^{2+}. The modest N lobe chemical shift changes upon Ca^{2+} titration suggest that the androcam N lobe remains closed. To identify the associated conformational change, we determined the androcam structure at a $CaCl_2$ level that drives Ca^{2+} binding to the N lobe. High-quality spectra were achieved at 10 mM $CaCl_2$, where the N lobe is approximately 70% occupied with Ca^{2+}. The single set of observed resonances (BioMagResBank: 17354) (17) shows that binding is in fast exchange, so our data report on a time-averaged Ca^{2+}-free and Ca^{2+}-bound N lobe, with the bound state dominating. In structures calculated without an explicit N lobe Ca^{2+} ion but with more than 5,000 experimental restraints measured at high Ca^{2+} (PDB 2LMU) (*SI Materials and Methods*), the Lys26 backbone carbonyl and Asp20, Thr24, and Gln62 side chain oxygens form a binding pocket. Adding a Ca^{2+} ion with distance restraints to these four oxygens in a second round of ARIA calculations gives the structures (Table S1) we discuss here, which indicate that the Glu22 side chain may also participate in metal binding. No significant differences are seen between the high and low Ca^{2+} androcam C lobes (Cα rmsd 1.08 Å). The high and low Ca^{2+} N lobes also superimpose well (Cα rmsd 1.15 Å, Fig. 4*A*) but residues 21–26 of the first EF loop move slightly toward the second EF loop at high Ca^{2+}. Thus, N lobe Ca^{2+} binding causes a small local change and not the global rearrangement seen in calmodulin.

The Single-Androcam N-Lobe Metal-Binding Site Includes Residues From Two EF Hands. The Gln62 side chain in the second EF hand points away from the Ca^{2+} binding pocket at low calcium but toward it at high calcium (Fig. 4*B*), indicating that residues from two EF hands form a single metal-binding site. Titration with $MgCl_2$ induces similar chemical shift changes that give $K_D \sim 6$ mM, consistent with optical titrations that detected no N-lobe Ca^{2+} binding in 6 mM $MgCl_2$ (11). Based on cellular

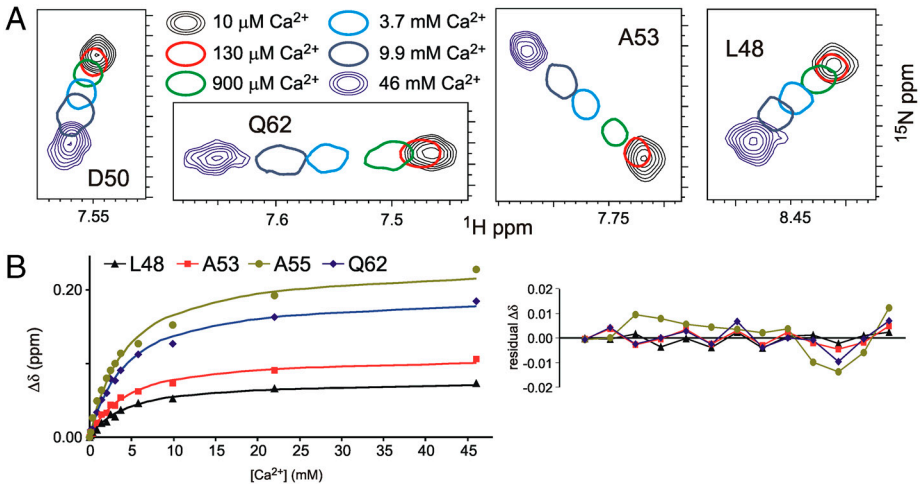

Fig. 2. $CaCl_2$ titration of androcam N lobe. (*A*) Selected peaks from androcam 2D ^{15}N HSQC spectra acquired at 10 μM, 130 μM, 900 μM, 3.7 mM, 9.9 mM and 46 mM $CaCl_2$. Seven additional spectra at intermediate $CaCl_2$ concentrations are included in the binding analysis. Chemical shift scales and contour levels are the same in all panels. All peak contours are shown for the endpoint spectra, but only the lowest contours are shown at intermediate points. (*B*) Smooth lines represent one single-site binding global fit to the experimental shifts as a function of $CaCl_2$. The best-fit model uses one global value of K_D (4.1 mM) and a free parameter for the maximal shift change of each peak. The difference between the model and experiment are shown at *Right*.

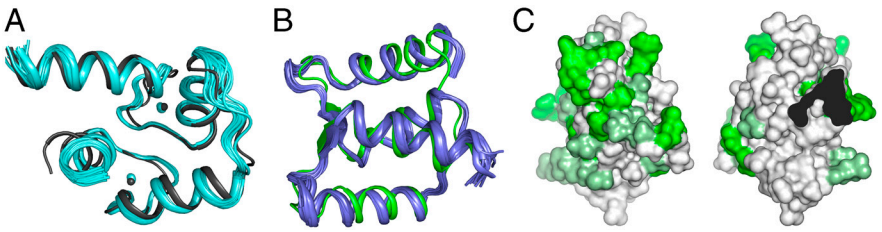

Fig. 3. Androcam structure at physiological calcium (2LMT). (*A*) 20 androcam C-lobe structures (cyan) superimposed on one another using Cα atoms (rmsd = 0.18 Å) and on holo-calmodulin C lobe (1CLL, gray) using Cα atoms of helices (rmsd = 1.45 Å). (*B*) 20 androcam N-lobe structures (slate) superimposed on one another using Cα atoms (rmsd = 0.23 Å) and on the calmodulin N lobe bound at the pig myosin VI IQ motif (3GN4, green) using Cα atoms of helices (rmsd = 1.41 Å). (*C*) Androcam N-lobe surface is white if residues match calmodulin and pale (bright) green if substitutions are conservative (non-conservative) based on BLOSUM62 scores from −3 to −6 (−8 to −13). Most changes cluster away from where the linker joins the N lobe (the black region in the view at *Right*).

Mg^{2+} and Ca^{2+} levels, this site is probably occupied by Mg^{2+} in vivo. Noncanonical metal binding has been seen for the closed calmodulin N lobe bound to edema factor (18), which has a fold similar to the androcam N lobe (Cα rmsd 1.63 Å) and binds a single metal using four residues of the first EF hand. Metal binding to calmodulin-like proteins does not always induce a change to the open state: The N lobe of the neuron-specific calcium binding protein 1 is closed despite one of the two N-lobe EF hands binding Ca^{2+} (19).

The Androcam N Lobe Does Not Bind Drosophila Myosin VI Insert 2. We assessed binding of both androcam and Drosophila calmodulin to a Drosophila myosin VI Insert 2 peptide (8) using NMR chemical shift changes. In calmodulin, Insert 2 peptide induces large shift changes for all backbone amides (Fig. 5*A*), indicating that both lobes bind and undergo global structural changes. We infer that the 1–14 binding mode seen for calmodulin at Insert 2 in pig myosin VI crystal structures (10, 16) is conserved in Drosophila. In androcam, Insert 2 peptide induces small shift changes for C-lobe amides and none for N-lobe amides (Fig. 5*B* and Fig. S2), indicating that androcam does not adopt the 1–14 binding mode. We infer that androcam binds Insert 2 with its C lobe only, explaining the higher affinity of calmodulin for this peptide (8).

Androcam Binds the Drosophila Myosin VI Regulatory IQ Site at all Ca^{2+} Levels. A Drosophila myosin VI IQ peptide (8) induces large chemical shift changes in all calmodulin amides (Fig. 6*A*), indicating that both lobes bind the peptide and undergo global structural changes. The same peptide induces small shift changes in androcam C-lobe but not N-lobe amides in the presence of excess $CaCl_2$ (Fig. 6*B*), indicating that the androcam C-lobe structure changes slightly upon binding the target but that the N lobe does not. We propose that the androcam N lobe contacts IQ without changing conformation because its structure in free solution mimics the calmodulin N lobe bound at the myosin VI IQ site (1.41 Å rmsd, Fig. 3*B*). This hypothesis is supported by the observation that deleting the androcam N lobe weakens IQ peptide binding 50-fold (8). Strikingly, 10 mM excess EDTA does not affect the androcam C-lobe peaks that shift on binding IQ (Fig. S3), showing that this lobe binds the target at high or low Ca^{2+}.

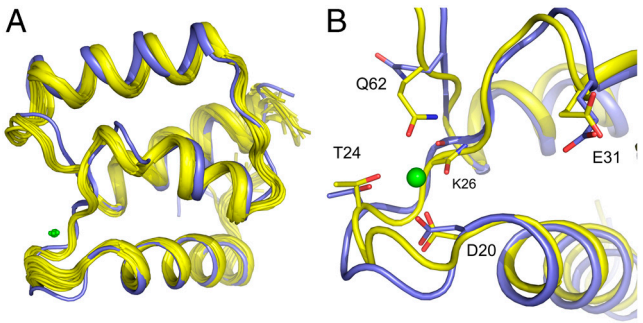

Fig. 4. Androcam structure at elevated calcium. (*A*) N lobes of the 20 lowest energy androcam structures in high calcium (yellow; 2LMV) superimposed on the lowest energy androcam structure in low calcium (slate) show that the helices do not move (Cα rmsd 1.15 Å). (*B*) N-lobe metal binding site of the lowest energy structure in low calcium (slate; 2LMT) and high calcium (yellow). Residues inferred to bind Ca^{2+} are shown except Glu22, which is omitted for clarity. Gln62 points into the binding pocket only at high calcium.

Calmodulin Forms a Well-Ordered Complex With Drosophila Myosin VI IQ Only at Intermediate Calcium Levels. Unlike androcam/IQ, calmodulin/IQ NMR spectra are strongly influenced by the availability of Ca^{2+}. Binding to the IQ peptide at two Ca^{2+} equivalents induces shift changes of all apo-calmodulin backbone amides (Fig. S4) and causes the C-lobe downfield glycine amides to appear (Fig. 7*B*). The downfield glycine shifts are consistent with calmodulin adopting the "semiopen Ca_2-C-lobe, closed apo-N-lobe" state seen at the IQ site of the pig myosin VI lever arm complex (16). As $[CaCl_2]$ is increased, the N lobe glycine peaks broaden, disappear, and then reappear at shifts similar to those of holo-calmodulin (Fig. 7*D*). In the presence of the IQ peptide and excess calcium, many calmodulin amides show multiple peaks indicating the presence of multiple conformations in slow exchange (Fig. S4). We infer that Ca^{2+} induces the calmodulin N lobe to open and destabilizes the closed apo-N lobe bound to IQ.

The Androcam N Lobe Does Not Bind a Canonical Calmodulin Target. We hypothesize that its constitutively closed N lobe prevents androcam from binding to canonical calmodulin target sites. We tested this idea with a skeletal muscle myosin light chain kinase (MLCK) peptide that binds to both lobes of calmodulin and induces large chemical shift changes for all backbone amides relative to Ca^{2+}-calmodulin (4). Titrating androcam with this peptide induces small shift changes for C-lobe amides only (Fig. S5), showing that the N lobe does not contact the target and providing an explanation for weak androcam binding to MLCK targets (11). The inability of Ca^{2+} or classic helical calmodulin targets like the MLCK and Insert 2 peptides to induce the androcam N lobe to open supports our hypothesis that androcam cannot adopt the archetypal calmodulin 1–14 or 1–10 binding modes (5).

Discussion

Myosin VI moves towards the pointed end of actin filaments and can act as an anchor on actin structures (20, 21). In mammals, two calmodulin molecules serve as myosin VI light chains, binding to the lever arm Insert 2 and IQ regions (9); calmodulin at the IQ site is thought to be regulatory, whereas at the Insert 2 site it is structural (9). Light chain binding is thought to rigidify the long, helical myosin lever arms that amplify motions generated by motor domain ATP hydrolysis into large steps (21, 22).

In *D. melanogaster*, myosin VI is critical to spermatogenesis (23, 24) where it stabilizes the mobile cone-shaped actin structures that mediate spermatid individualization. Myosin VI accumulates at the leading edge of the cones and is required for the

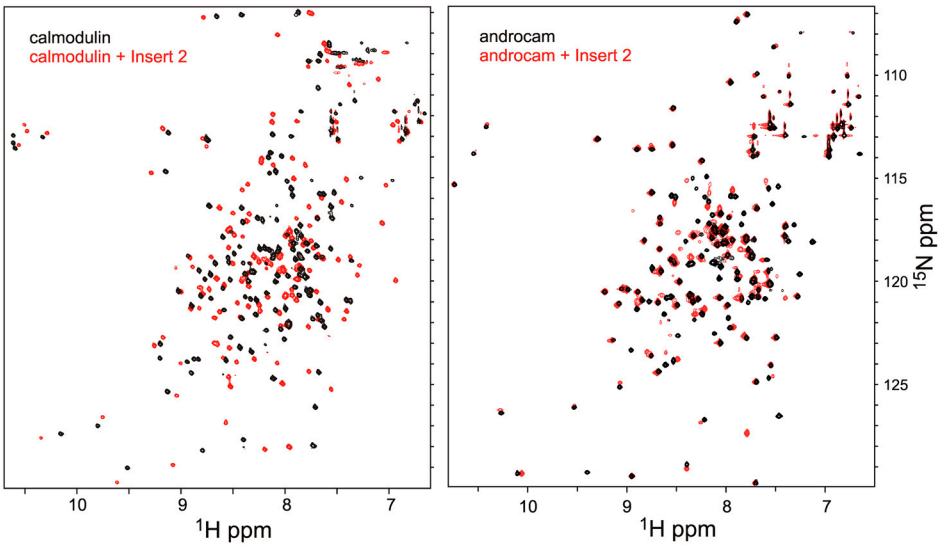

Fig. 5. Insert 2 peptide titrations of calmodulin and androcam. ^{15}N HSQC spectra for calmodulin (*A*) and androcam (*B*) alone (black) and with equimolar fly myosin VI Insert 2 peptide (red). Calmodulin amide chemical shifts from both lobes are perturbed; only androcam C lobe amides show any changes (see Fig. S2 for androcam peak assignments). Data acquired at 800 MHz on 260 μM ^{15}N-labeled calmodulin (10 mM $CaCl_2$, 10 mM KCl, 10 mM Tris-HCl, pH 7.2, 25 °C) or 385 μM ^{15}N-labeled androcam (10 mM $CaCl_2$, 10 mM KCl, 10 mM Tris-HCl, 10 mM DTT, pH 7.4, 25 °C).

correct localization of the actin regulators cortactin and arp2/3 (24–26). The myosin VI-dependent presence of androcam on the cones (8) suggests that this light chain bestows functional properties on myosin VI distinct from those conferred by calmodulin, and our data show that androcam interacts differently than calmodulin with the myosin VI Insert 2 and IQ sites.

Light chain structure and target binding differences arise largely from the androcam N lobe, which is closed under all conditions even though threading onto calmodulin open N lobes (1CLL, 2O5G, 3GN4) did not identify steric clashes that might block lobe opening or target binding. Changes to Ca^{2+}-coordinating residues in the first and second EF hands, especially Asp26Thr, favor a closed N lobe by decreasing Ca^{2+}-induced stabilization of the open form. Unexpectedly, androcam Gln62 of the second EF hand cooperates with residues of the first EF hand to coordinate Ca^{2+} (or Mg^{2+}) in the closed state, thus breaking the usual EF-hand paradigm in which Ca^{2+} preferentially stabilizes the open state. The unique androcam N-lobe structure determines previously undescribed interaction modes with myosin VI and also prevents canonical binding to other calmodulin cellular targets, thus explaining how the testis-specific expression of androcam provides a specialized myosin VI light chain without misregulation of other calmodulin targets.

We model light chain binding to Drosophila myosin VI based on structures of calmodulin bound to pig myosin VI fragments at Insert 2 and IQ sites (10, 16). Androcam binds tightly to both Insert 2 and IQ motifs of Drosophila myosin VI (8), so we expect that two androcam molecules bind myosin VI in vivo. Our data show that whereas Drosophila calmodulin binds the Drosophila myosin VI light chain sites much as in mammals, androcam binding at both these sites is quite different.

Our demonstration that androcam binds at the Insert 2 site with its C lobe only suggests that the stiffness of the lever arm will decrease compared to when calmodulin is the light chain. Increased lever-arm flexibility will alter the processive stepping and load-induced anchoring properties of the motor because the rigid lever arms are thought to transmit mechanical tension that couples the nucleotide- and actin-binding properties of the catalytic domains in a myosin VI dimer (27–30).

Tethering the closed androcam N lobe at Insert 2 by its C lobe could itself affect myosin VI function. The N lobe patch of nonconserved androcam residues (Fig. 3*C*) could mediate protein–protein interactions distinct from those supported by calmodulin, perhaps contributing to myosin VI-dependent actin cone accumulation of cortactin and arp2/3 (24–26) or other targets (31). A similar role in recruiting partners has been proposed for N lobes of light chains that bind only through their C lobes to certain IQ motifs of the myosin V lever arm (32, 33). The free androcam N lobe could also stabilize the monomeric form of myosin VI thought to function on actin cones (34) by contacting

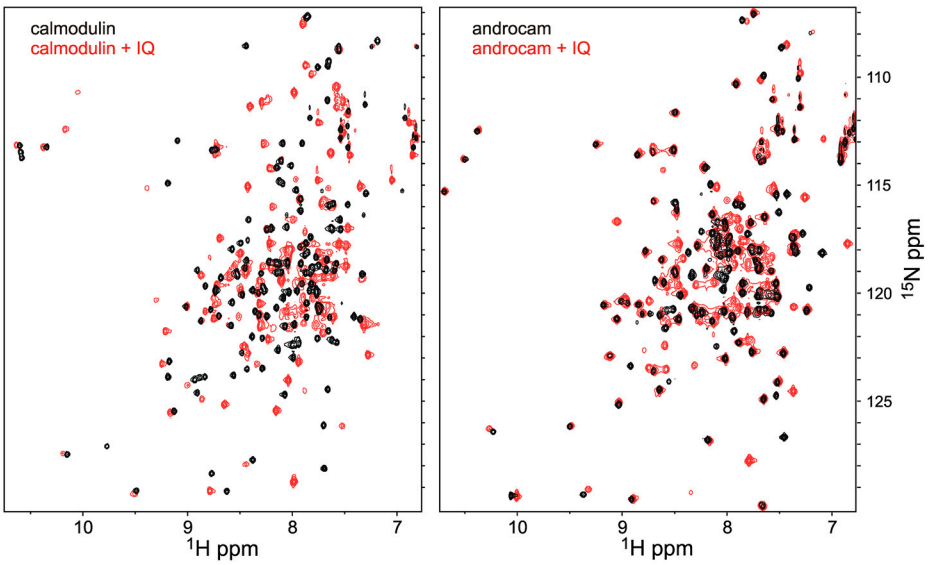

Fig. 6. IQ peptide titrations of calmodulin and androcam. (*A*) ^{15}N HSQC spectra of Ca_4-calmodulin (black) and Ca_2-calmodulin with equimolar fly myosin VI IQ peptide (red); resonances from both lobes show significant chemical shift changes. (*B*) ^{15}N HSQC spectra of androcam alone (black) and with equimolar fly myosin VI IQ peptide (red); only androcam C lobe amides show modest changes (Fig. S3). Data acquired at 800 MHz on 250 μM ^{15}N-labeled calmodulin (80 mM KCl, 10 mM Tris-HCl, 5 mM DTT, pH 7.4, 25 °C; Ca_4-calmodulin in 10 mM $CaCl_2$, Ca_2-calmodulin by titration from apo-calmodulin) or 400 μM ^{15}N-labeled androcam (10 mM $CaCl_2$, 10 mM KCl, 10 mM Tris-HCl, 5 mM DTT, pH 7.4, 25 °C).

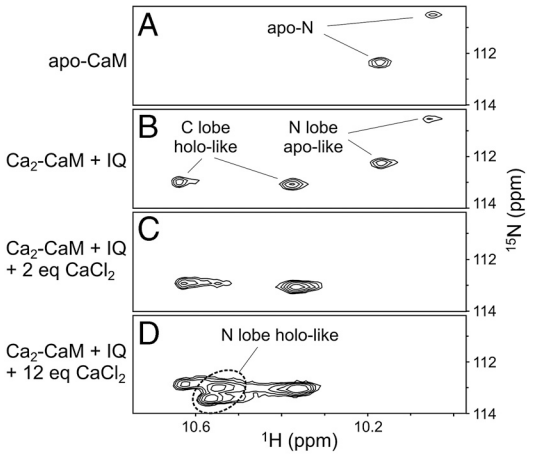

Fig. 7. Calmodulin downfield glycine amide shifts indicate the conformation each lobe adopts when interacting with IQ peptide and Ca^{2+}. Apo-calmodulin (*A*) does not show C-lobe downfield glycines due to conformational exchange. Adding IQ peptide and 2 $CaCl_2$ equivalents generates a well-defined species with apo-N- and holo-C-like EF-hand glycine shifts (*B*). Two more $CaCl_2$ equivalents broaden the N-lobe glycines beyond detection (*C*); a large excess of $CaCl_2$ (3 mM) drives the N-lobe glycines to shifts very similar to holo-calmodulin. Data acquired at 800 MHz on 250 μM ^{15}N-labeled calmodulin (80 mM KCl, 10 mM Tris-HCl, 5 mM DTT, pH 7.4, 25 °C).

the C-terminal cargo-binding region of myosin VI monomer and helping it remain folded back on the catalytic domain (35). We propose that N-lobe interactions with the motor or other cone components allow androcam to displace calmodulin from the actin cones despite its weaker affinity for Insert 2 in isolation (8).

Our demonstrations that androcam binds the IQ site constitutively whereas calmodulin/IQ interactions are regulated by Ca^{2+} lead us to propose that androcam converts a regulated myosin VI property to a constitutive one. A three-helix bundle at the distal end of the myosin VI lever arm is thought to unfold upon motor dimerization, extending the lever arm and making possible the 36 nm dimer step size (16). Calmodulin at the pig myosin VI IQ site interacts with this bundle through its N lobe (Fig. 8*A*), and the Ca^{2+}-free N lobe may maintain contacts with the first helix after the bundle unfolds (16) (Fig. 8*B*). We propose that Ca^{2+} binding to the N lobe drives it to an open state and disrupts these contacts, which encourages the bundle to unfold, altering the lever arm in a Ca^{2+}-dependent way (Fig. 8*C*). Consistent with this proposal, the apo-calmodulin-like N-lobe downfield glycine peaks in the presence of IQ peptide move to chemical shifts similar to those of holo-calmodulin in excess $CaCl_2$ (Fig. 7). This regulated coupling of Ca^{2+} binding to lever arm extension is abolished when androcam is the light chain (Fig. 8*D*) because its N lobe interactions will be constitutive.

It is informative to consider how calmodulin-like proteins might arise, especially since changes in calmodulin are so disfavored by evolution that the human and Drosophila proteins differ by only three residues. If gene duplication places a copy of calmodulin behind a tissue-specific promoter, and this elevated calmodulin expression improves organismal fitness, then the copy will fix in the population. The original, ubiquitously expressed calmodulin gene experiences strong selective pressure to maintain its sequence because changes would alter many functional readouts in different tissues, and the chance of all these simultaneous changes being net beneficial is vanishingly small. However, the tissue-specific copy will experience selective pressures related only to its function in that particular tissue. Changes that do not abolish the evolutionary fitness imparted via that tissue would be silent, and those that improve fitness would be positively selected.

Consistent with this hypothetical scenario, the androcam gene is part of a cluster of intronless calmodulin-like open reading frames that is conserved within the Drosophila genus and postulated to have arisen by retrotransposition and gene duplication (7). In mammals and Drosophila, genes derived by retrotransposition often show testis-specific expression, and although the underlying mechanisms are not understood, acquiring molecular functionality in sperm is a common step in the evolution of many new genes (36). Drosophila species produce enormously long sperm (1.8 mm in *D. melanogaster*) whose proper formation requires the androcam/myosin VI complex on the actin cones. We speculate that the fortuitous production of a testis-specific calmodulin-like protein and its co-evolution with myosin VI led to a light chain/motor pair that could support the unusual processes necessary to generate these giant gametes. Myosin VI is a unique gene in Drosophila with only one protein isoform, so it must interact functionally with calmodulin in most instances and with androcam in spermatogenesis. Differences between fly and mammalian myosin VI light chain-binding regions may therefore represent functional adaptations rather than neutral drift.

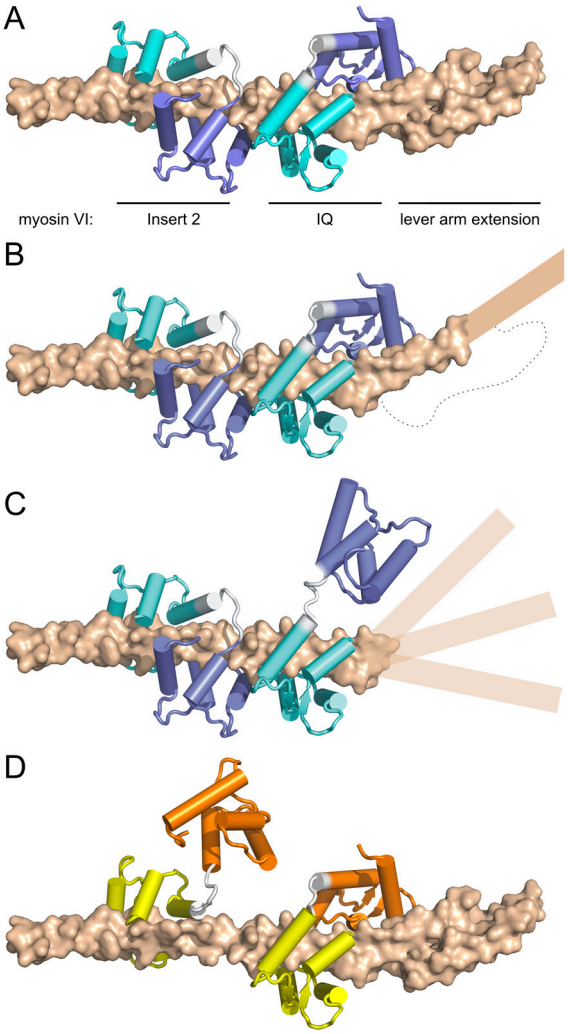

Fig. 8. Structure and models for light chain binding to myosin VI. Calmodulin N lobes are slate, linkers are white, C lobes are aqua, and the myosin VI lever arm is brown. (*A*) In structure 3GN4 (16), calmodulin binds at Insert 2 in a compact mode (*Left*) and at IQ in a mode that contacts the three helix bundle (*Right*). (*B*) Model (16) in which bundle unfolding extends the lever arm, perhaps in the direction stabilized by the calmodulin N lobe contacting the first helix. (*C*) We propose that Ca^{2+} binding switches the calmodulin N lobe to the open state, releasing the bundle to reorient and/or extend. (*D*) In our androcam/myosin VI model, androcam binds Insert 2 with its C lobe (yellow), and its N lobe (orange) is free to interact elsewhere; androcam binds IQ and the lever arm extension at all Ca^{2+} concentrations.

Why are there so many calmodulin-like proteins? Any duplicated gene can yield a functionally distinct variant, but calmodulin is structurally plastic: It samples many states and binds to diverse targets in a variety of modes. Almost any mutation in a duplicate calmodulin gene would favor some binding interactions over others, generating functional differences upon which selection could act. In contrast, other genes might need many mutations to generate a new binding mode that could alter biological function. We propose that tissue-specific calmodulin variants will, like androcam, have lost much of the versatility of calmodulin in favor of specialized structures and functions because they have escaped the stalemate of offsetting selective pressures to which calmodulin is subject. Their structures will likely be similar to one of the states that calmodulin adopts, although unique interaction surfaces may be recruited and properties may be dramatically altered with minimal sequence changes: Androcam is 67% identical to calmodulin, but its N lobe has evolved a unique metal binding mode that stabilizes the closed state. Calmodulin-like proteins may each be functionally unique by adopting just one of the many modes that their versatile ancestor calmodulin uses to bind targets.

Materials and Methods

Labeled androcam was prepared to give samples at 10 μM or 10 mM free Ca^{2+} as described (13, 17). Standard NMR methods were used to identify every backbone HN, N, C′, C_α, and C_β chemical shift, all aliphatic protons, and >99% of nonexchangeable protons as described (13, 17). $^3J_{HNH\alpha}$ couplings (37) were used quantitatively in the low Ca^{2+} structure and qualitatively in the high Ca^{2+} structure. Three-dimensional HNHB and HNCOHB spectra (37) were used to stereospecifically assign Hβs and assign χ_1 rotamers. For the low Ca^{2+} structure, $^3J_{CN}$ and $^3J_{CC'}$ (37) couplings to γ methyl carbons were used to assign Val, Ile, and Thr χ_1 rotamers and stereospecifically assign Val methyls, and $^3J_{C\alpha C\delta}$ couplings from 3D LRCC (37) or 2D difference (38) spectra were used to assign Leu and Ile χ_2 rotamers and stereospecifically assign Leu methyls. Analysis of C_α, C′, H_α, and C_β chemical shifts (39) was used to identify secondary structure elements and to generate hydrogen bond and φ, ψ dihedral restraints. Structure determination was performed using ARIA 1.2 (14). All NOE peak assignments were made by ARIA without human intervention. The 20 lowest energy structures of 50 calculated in the last round of ARIA were used for analysis. Chemical shift assignments for androcam and high Ca^{2+} androcam have been deposited in BioMagResBank, accession codes 17353 and 17354. Coordinates and restraints are deposited under accession codes 2LMT for androcam and 2LMU and 2LMV for high Ca^{2+} androcam. Drosophila Insert 2 peptide (AKVKKWLIRSRWVKSALGALCVIKLRNRI) and IQ peptide (YRNKCVLIAQRIARGFLARKQHRPRYQ) were N-acetylated and C-amidated, as in prior binding studies (8).

ACKNOWLEDGMENTS. The authors thank the MacKenzie, Beckingham, and Shamoo groups for advice and Clinton Heider for LINUX support. K.M.B. acknowledges support from National Institutes of Health Grant HD39766 and Welch Foundation Grant C-1119.

1. Babu YS, et al. (1985) Three-dimensional structure of calmodulin. *Nature* 315:37–40.
2. Barbato G, Ikura M, Kay LE, Pastor RW, Bax A (1992) Backbone dynamics of calmodulin studied by ^{15}N relaxation using inverse detected two-dimensional NMR spectroscopy: The central helix is flexible. *Biochemistry* 31:5269–5278.
3. Meador WE, Means AR, Quiocho FA (1992) Target enzyme recognition by calmodulin: 2.4 Å structure of a calmodulin-peptide complex. *Science* 257:1251–1255.
4. Ikura M, et al. (1992) Solution structure of a calmodulin-target peptide complex by multidimensional NMR. *Science* 256:632–638.
5. Hoeflich KP, Ikura M (2002) Calmodulin in action: Diversity in target recognition and activation mechanisms. *Cell* 108:739–742.
6. Lu AQ, Beckingham K (2000) Androcam, a Drosophila calmodulin-related protein, is expressed specifically in the testis and decorates loop kl-3 of the Y chromosome. *Mech Dev* 94:171–181.
7. Pavlik P, Konduri V, Massa E, Simonette R, Beckingham KM (2006) A dicistronic gene pair within a cluster of "EF-hand" protein genes in the genomes of Drosophila species. *Genomics* 88:347–359.
8. Frank DJ, et al. (2006) Androcam is a tissue-specific light chain for myosin VI in the Drosophila testis. *J Biol Chem* 281:24728–24736.
9. Bahloul A, et al. (2004) The unique insert in myosin VI is a structural calcium–calmodulin binding site. *Proc Natl Acad Sci USA* 101:4787–4792.
10. Menetrey J, et al. (2005) The structure of the myosin VI motor reveals the mechanism of directionality reversal. *Nature* 435:779–785.
11. Martin SR, et al. (1999) Conformational and metal-binding properties of androcam, a testis-specific, calmodulin-related protein from Drosophila. *Protein Sci* 8:2444–2454.
12. Clapham DE (2007) Calcium signaling. *Cell* 131:1047–1058.
13. Joshi MK, Moran S, MacKenzie KR (June 17, 2012) NMR chemical shift assignments for androcam, a testis-specific myosin VI light chain in *D melanogaster. Biomol NMR Assign*, 10.1007/s12104-012-9402-1.
14. Linge JP, Habeck M, Rieping W, Nilges M (2003) ARIA: Automated NOE assignment and NMR structure calculation. *Bioinformatics* 19:315–316.
15. Holm L, Rosenstrom P (2010) Dali server: Conservation mapping in 3D. *Nucleic Acids Res* 38:W545–W549.
16. Mukherjea M, et al. (2009) Myosin VI dimerization triggers an unfolding of a three-helix bundle in order to extend its reach. *Mol Cell* 35:305–315.
17. Joshi MK, Moran S, MacKenzie KR (June 17, 2012) ^1H, ^{15}N and ^{13}C chemical shifts of the D. *melanogaster* myosin VI light chain androcam in high calcium. *Biomol NMR Assign*, 10.1007/s12104-012-9403-0.
18. Shen Y, Zhukovskaya NL, Guo Q, Florian J, Tang WJ (2005) Calcium-independent calmodulin binding and two-metal-ion catalytic mechanism of anthrax edema factor. *EMBO J* 24:929–941.
19. Park S, Li C, Ames JB (2011) Nuclear magnetic resonance structure of calcium-binding protein 1 in a Ca^{2+}-bound closed state: Implications for target recognition. *Protein Sci* 20:1356–1366.
20. Sweeney HL, Houdusse A (2007) What can myosin VI do in cells? *Curr Opin Cell Biol* 19:57–66.
21. Spudich JA, Sivaramakrishnan S (2010) Myosin VI: An innovative motor that challenged the swinging lever arm hypothesis. *Nat Rev Mol Cell Biol* 11:128–137.
22. Holmes KC (1997) The swinging lever-arm hypothesis of muscle contraction. *Curr Biol* 7:R112–118.
23. Hicks JL, Deng WM, Rogat AD, Miller KG, Bownes M (1999) Class VI unconventional myosin is required for spermatogenesis in Drosophila. *Mol Biol Cell* 10:4341–4353.
24. Rogat AD, Miller KG (2002) A role for myosin VI in actin dynamics at sites of membrane remodeling during Drosophila spermatogenesis. *J Cell Sci* 115:4855–4865.
25. Noguchi T, Lenartowska M, Miller KG (2006) Myosin VI stabilizes an actin network during Drosophila spermatid individualization. *Mol Biol Cell* 17:2559–2571.
26. Noguchi T, Lenartowska M, Rogat AD, Frank DJ, Miller KG (2008) Proper cellular reorganization during Drosophila spermatid individualization depends on actin structures composed of two domains, bundles and meshwork, that are differentially regulated and have different functions. *Mol Biol Cell* 19:2363–2372.
27. Altman D, Sweeney HL, Spudich JA (2004) The mechanism of myosin VI translocation and its load-induced anchoring. *Cell* 116:737–749.
28. Dunn AR, Chuan P, Bryant Z, Spudich JA (2010) Contribution of the myosin VI tail domain to processive stepping and intramolecular tension sensing. *Proc Natl Acad Sci USA* 107:7746–7750.
29. Nishikawa S, et al. (2010) Switch between large hand-over-hand and small inchworm-like steps in myosin VI. *Cell* 142:879–888.
30. Chuan P, Spudich JA, Dunn AR (2011) Robust mechanosensing and tension generation by myosin VI. *J Mol Biol* 405:105–112.
31. Finan D, Hartman MA, Spudich JA (2011) From the cover: Proteomics approach to study the functions of Drosophila myosin VI through identification of multiple cargo-binding proteins. *Proc Natl Acad Sci USA* 108:5566–5571.
32. Terrak M, Rebowski G, Lu RC, Grabarek Z, Dominguez R (2005) Structure of the light chain-binding domain of myosin V. *Proc Natl Acad Sci USA* 102:12718–12723.
33. Terrak M, Wu G, Stafford WF, Lu RC, Dominguez R (2003) Two distinct myosin light chain structures are induced by specific variations within the bound IQ motifs-functional implications. *EMBO J* 22:362–371.
34. Noguchi T, Frank DJ, Isaji M, Miller KG (2009) Coiled-coil-mediated dimerization is not required for myosin VI to stabilize actin during spermatid individualization in Drosophila melanogaster. *Mol Biol Cell* 20:358–367.
35. Spink BJ, Sivaramakrishnan S, Lipfert J, Doniach S, Spudich JA (2008) Long single alpha-helical tail domains bridge the gap between structure and function of myosin VI. *Nat Struct Mol Biol* 15:591–597.
36. Dorus S, Freeman ZN, Parker ER, Heath BD, Karr TL (2008) Recent origins of sperm genes in Drosophila. *Mol Biol Evol* 25:2157–2166.
37. Bax A, et al. (1994) Measurement of homo- and heteronuclear J couplings from quantitative J correlation. *Methods Enzymol* 239:79–105.
38. MacKenzie KR, Prestegard JH, Engelman DM (1996) Leucine side-chain rotamers in a glycophorin A transmembrane peptide as revealed by three-bond carbon–carbon couplings and ^{13}C chemical shifts. *J Biomol NMR* 7:256–260.
39. Wishart DS, Sykes BD (1994) The ^{13}C chemical-shift index: A simple method for the identification of protein secondary structure using ^{13}C chemical-shift data. *J Biomol NMR* 4:171–180.
40. Ataman ZA, Gakhar L, Sorensen BR, Hell JW, Shea MA (2007) The NMDA receptor NR1 C1 region bound to calmodulin: Structural insights into functional differences between homologous domains. *Structure* 15:1603–1617.